Far-Infrared Spectroscopy

DOI: 10.1002/ange.201102014

Profiling the Active Site of a Copper Enzyme through Its Far-Infrared Fingerprint**

Laure Marboutin, Hugo Petitjean, Bertrand Xerri, Nicolas Vita, François Dupeyrat, Jean-Pierre Flament, Dorothée Berthomieu, and Catherine Berthomieu**

Present in all eukaryotic cells, the Cu,Zn-superoxide dismutase enzyme (Cu,Zn-SOD) plays a key role in the protection of cells against aging caused by superoxide and deriving reactive oxygen species. Dismutation of superoxide ($O_2^{-\bullet}$) into dioxygen and hydrogen peroxide is catalyzed by Cu,Zn-SOD at one of the fastest enzyme rates (around $10^9\,\text{M}\,\text{s}^{-1}$).[1–3] Dismutation of $O_2^{-\bullet}$ directly involves the redox Cu^{II}/Cu^{I} center [Eqs. (1) and (2)]. Dismutation mechanisms were

$$[Cu^{II}] + O_2^{-\bullet} \rightarrow [Cu^{I}] + O_2 \quad (1)$$

$$[Cu^{I}] + O_2^{-\bullet} + 2\,H^+ \rightarrow [Cu^{I}] + H_2O_2 \quad (2)$$

proposed from high-resolution structures of the reduced/oxidized enzyme,[4–7] but the mechanism of the reduction step [Eq. (2)] is still under debate[4,6–8] because characterizations of the active site diverge about the coordination sphere of the Cu^{I} center.[6,9,10] Characterization of the active sites remains an experimental challenge for all enzymatic issues and puts two questions: how can the molecular motifs of the active site be distinguished from the rest of the protein and how can these motifs be characterized in each reactive state of the protein in solution? In this study, we show how infrared (IR) spectroscopy in the low-frequency domain, targeting metal–ligand bond properties, can address these general issues in the case of Cu,Zn-SOD.

[*] Dr. L. Marboutin, Dr. N. Vita, Dr. F. Dupeyrat, Dr. C. Berthomieu
CEA, DSV, IBEB, Lab Interact Protein Metal
CNRS, UMR 6191 Biol Veget and Microbiol Environ
Aix-Marseille Université, 13108 Saint-Paul-lez-Durance (France)
E-mail: catherine.berthomieu@cea.fr
Dr. H. Petitjean, Dr. B. Xerri, Dr. D. Berthomieu
Institut Charles Gerhardt, MACS
UMR 5253 CNRS-ENSCM-UM1-UM2
8, rue de l'Ecole Normale, 34296 Montpellier cedex 5 (France)
E-mail: bertho@univ-montp2.fr
Dr. J.-P. Flament
Université Lille 1, Sciences et Technologies
Laboratoire de Physique des Lasers
Atomes et Molécules (UMR, CNRS 8523)
and CERLA (FR 2416 CNRS)
59655 Villeneuve d'Ascq Cedex (France)

[**] This work was funded in part by the French Agence Nationale de la Recherche (grant number ANR-08-PCVI-0011). D.B. acknowledges the Centre Informatique National de l'Enseignement Supérieur (CINES) and the Toxicologie Nucléaire Environnementale Programme.

Supporting information for this article is available on the WWW under http://dx.doi.org/10.1002/anie.201102014.

Properties of the Cu^{I},Zn-SOD active site were barely studied in solution by spectroscopy, excepted by NMR spectroscopy.[11–15] The diamagnetic Cu^{I} state is not accessible to ESR spectroscopy, and does not absorb in the visible domain, which prevents UV/Vis and Vis/resonance Raman spectroscopies. In principle, bonds of the Cu,Zn-SOD active site could be characterized with vibrational spectroscopy, but, in practice, IR spectroscopists face two difficulties. First, most of the metal–ligand vibrations contribute in the far-IR region (below $500\,\text{cm}^{-1}$) and cannot be caught with conventional FTIR spectroscopy. Second, because literature has never reported far-IR vibrational spectra of copper proteins, spectra of Cu,Zn-SOD have to be assigned from scratch.

Herein, we present the first far-IR investigation on a copper protein, Cu,Zn-SOD. We specifically probed the Cu,Zn-SOD active site by coupling FTIR spectroscopy to the electrochemical switch between Cu^{II} and Cu^{I} states: this high-resolution technique provides difference spectra that keep only vibrational signals sensitive to the Cu^{II}/Cu^{I} switch. Up to recently, far-IR data on metalloproteins were reported for light-induced FTIR difference spectra on photosystem II down to $300\,\text{cm}^{-1}$ and on the Rieske protein.[16–21] Our electrochemically induced far-IR difference spectra were recorded in aqueous solution down to wavenumbers of $50\,\text{cm}^{-1}$.[22,23]

Besides this experimental accomplishment, our study aims at defining reliable IR marker for the active site and for tracking structural changes of this active site upon conversion of the Cu^{II}/Cu^{I} redox states and changes of the pH value.

In Cu^{II},Zn-SOD, the copper cation is coordinated to four histidines (His) arranged in a distorted tetragonal shape.[7,24,25] A water molecule forms a Cu^{II} pseudo-ligand, and one histidine (His_{61}) acts as a bridging ligand between the copper and zinc centers (Figure 1). The other ligands of the zinc center are two histidines and a monodentate aspartate.[7,24,25]

In Cu^{I},Zn-SOD, the bridging role of His_{61} was studied: maintenance of the bridge was observed in some crystal structures and in the presence of anions[9,26] but data recorded in solution and obtained from crystallographic studies showed that His_{61} solely coordinates the Zn center.[4,6,7,12,27–30] We also studied the influences of the Cu^{II}/Cu^{I} switch and the pH value on the water pseudo-ligand connected to a network of water molecules in the access channel of superoxide that may play a determining role in the reduction of superoxide.[6]

Electrochemically induced far-IR difference spectra of Cu,Zn-SOD (Figures 2–5) show well-defined and highly reproducible bands in the whole domain from 680 to $50\,\text{cm}^{-1}$. In the spectra, positive bands correspond to the

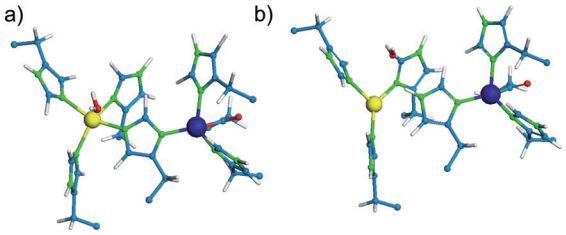

Figure 1. Structures 1E9Q and 1Q0E from the protein data bank of a) Cu^{II},Zn-SOD and b) Cu^{I},Zn-SOD active sites. The gray sticks are H atoms, blue spheres are C atoms, large yellow spheres are Cu atoms, red spheres are O atoms, green spheres are N, big dark-blue spheres are Zn atoms.

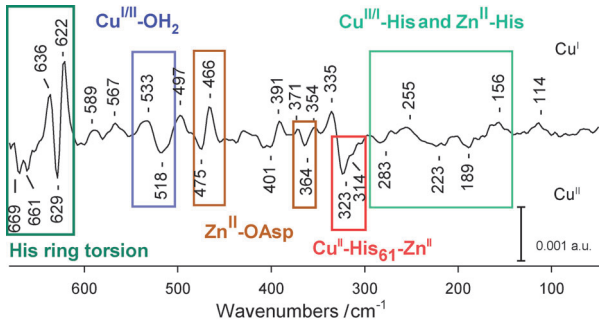

Figure 2. Low-frequency FTIR difference spectrum of the reduced minus oxidized (Cu^{I}/Cu^{II}) Cu center recorded for Cu,Zn-SOD at pH 9.3 in H_2O.

Cu^{I} state and negative bands correspond to the Cu^{II} state. Only bands influenced by the Cu^{II}/Cu^{I} switch are observed, that is, the IR contributions of aqueous medium and protein backbone are annihilated.

We assigned the difference spectra by a dual experimental and theoretical approach, supported by a thorough study of the isotopic shifts. FTIR spectra were recorded on Cu,Zn-SOD in H_2O, D_2O, and $H_2{}^{18}O$ to probe contributions from the exchangeable protons and from the water pseudo-ligand of the Cu^{II} center. Complementary FTIR spectra were recorded on Cu,Cd-SOD to probe metal–ligand vibrations influenced by substitution of Zn^{II} by Cd^{II}. The experimental frequencies were compared with those predicted from DFT modeling on Cu^{II},Zn-SOD and Cu^{I},Zn-SOD optimized cluster models (see the Supporting Information). The accordance of experimental and theoretical frequencies was supported by the accordance of experimental and modelled isotopic shifts induced by exchanges of H_2O/D_2O and $H_2O/H_2{}^{18}O$. The vibrational modes were analyzed through their potential-energy distribution (PED), which gives the relative contribution of each internal vibrational coordinate to the normal modes (see Tables S2 and S3 in the Supporting Information).

Histidine side chains provide two ring torsion modes that identify histidine–metal interactions. These modes are obtained from PED analysis, in agreement with data obtained from free and coordinated imidazole (see Table S2 in the Supporting Information).[23,31,32] These modes are intense, sensitive to the Cu valence state, and appear at 669, 661, 653, and 629 cm^{-1} for the Cu^{II} state and at 636 and 622 cm^{-1} for the Cu^{I} state (Figure 2). Because the calculated IR modes of Nπ and Nτ coordinated histidine are found in the same spectral range, these modes cannot be used to discriminate Nπ- from Nτ-metal coordination.

The $Zn–O_{Asp}$ metal–ligand bond contributes to two IR modes localized at 475 and 364 cm^{-1} (Cu^{II}) and at 466 and 371 cm^{-1} (Cu^{I}). Experimentally, these bands shift to lower frequencies upon substitution of Zn^{II} by Cd^{II} (Figure 3), and this observation supports the assumption of a contribution from the Zn^{II} coordination sphere. These bands correspond to the modes calculated at 473, 398, 394 cm^{-1} (Cu^{II}) and at 375 cm^{-1} (Cu^{I}) involving the $\nu(Zn–O_{Asp})$ stretching vibration (see Tables S2 and S3 in the Supporting Information).

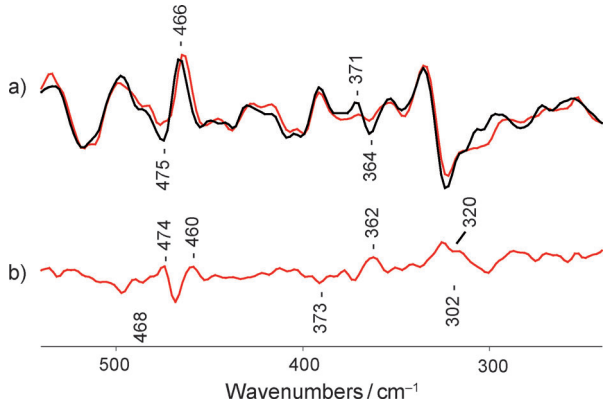

Figure 3. Low-frequency FTIR difference spectra of the reduced minus oxidized (Cu^{I}/Cu^{II}) Cu center recorded for a) Cu,Cd-SOD (red line) and Cu,Zn-SOD (black line) in H_2O at pH 9.3, b) difference calculated from spectra of Cu,Zn-SOD and Cu,Cd-SOD.

Modes involving large contributions from ν(Cu–His) and ν(Zn–His) vibrations are calculated below 350 cm^{-1}. Our discussion focuses on the informative IR marker mode of the bridging Cu^{II}-His_{61}-Zn motif. Assignment of the residual modes of the spectrum is detailed in the Supporting Information.

The bridging Cu-His_{61}-Zn motif can be clearly assigned to an IR mode of the Cu^{II} state. This mode is the negative band detected experimentally at 323 cm^{-1} with a shoulder at 314 cm^{-1} (Figure 2). Indeed, a part of this band shifts to lower frequency upon substitution of Zn^{II} by Cd^{II} (Figure 3). This mode corresponds to the most intense calculated Cu^{II} mode in this spectral region, predicted at 301 cm^{-1} and involving contributions of 23% from $\nu(Cu–N\tau(His_{61}))$ and 13% from $\nu(Zn–N\pi(His_{61}))$. From the calculations, bending modes involving Cu and its His ligands may also contribute to the broad experimental band at 323-314 cm^{-1} (see Tables S2 and S3 in the Supporting Information), which explains the downshift of only part of the band upon exchange of Zn by Cd.

The present far-IR investigation suggests that the Cu-His_{61}-Zn bridge is broken in the Cu^{I} state because the Cu-His_{61}-Zn marker mode appears solely for the Cu^{II} state. In this spectral range, no positive band corresponding to the Cu^{I} state was found that is sensitive to exchange of Zn^{II} by Cd^{II}.

The present results are in agreement with extended X-ray absorption fine structure (EXAFS), NMR, and UV-Raman spectroscopic observations showing that the Cu-His_{61}-Zn bridge is broken when Cu^{II},Zn-SOD turns into Cu^{I},Zn-SOD in solution.[11,28,30,33]

The modes of the water pseudo-ligand are especially informative about the properties of the Cu–water interactions. First, the modeling of these water modes gives insights in the properties of the Cu–OH_2 bond, and second, one of these modes provides a useful IR marker mode to track changes in this bond upon switching Cu^{I} to Cu^{II} state and upon pH variation.

Modes involving the ν(Cu–O) vibration are predicted to be found in the IR spectrum below 200 cm^{-1} (see Table S3 in the Supporting Information). These calculated frequencies are lower than those reported for various metal–water complexes which are located at 490 to 310 cm^{-1}.[34–36] Because the ν(Cu–O) frequency mode correlates with the strength of the Cu–O bond, the lower predicted frequencies indicate that in Cu^{II},Zn-SOD, the Cu–water interaction corresponds to a weak ionic interaction. This is consistent with coordination of water to Cu^{II} in axial position with a long Cu–OH_2 bond. Unfortunately, the ν(Cu–O) mode was not identified in the present far-IR spectra of Cu,Zn-SOD probably because of its weak intensity: experimental data below 300 cm^{-1} do not show significant shifts neither upon H_2O/D_2O nor upon $H_2{}^{16}O/H_2{}^{18}O$ exchange (see Figure 4 and Figure S3 in the Supporting Information), whereas calculations predicted downshifts by 4–10 and 2–3 cm^{-1}, respectively, for modes involving the ν(Cu–O) vibration (see Table S3 in the Supporting Information).

In contrast, IR modes indicative of water molecules bound to the active site of Cu,Zn-SOD are provided by the torsion and bending frequencies involving the water pseudo-ligand at around 520 cm^{-1} (Figure 2). The experimental bands at 533 (Cu^{I}) and 518 cm^{-1} (Cu^{II}) shift largely to lower frequencies upon H_2O/D_2O exchange to 410 or 347 cm^{-1} (Cu^{I}) and to 449 cm^{-1} (Cu^{II}) (Figure 4), respectively. Because no other IR mode downshift so largely in this spectral range (see the Supporting Information), we propose that these bands correspond to the calculated modes at 597 cm^{-1} (Cu^{I}) and 449 cm^{-1} (Cu^{II}), which shift by −159 cm^{-1} and −119 cm^{-1} upon H_2O/D_2O exchange (see Table S2 in the Supporting Information), respectively. The calculated mode at 597 cm^{-1} (Cu^{I}) involves τ(H-O-Cu-N_{His}) torsion, and the mode at 449 cm^{-1} (Cu^{II}) involves δ(H-O-Cu) wagging and τ(H-O-Cu-N_{His}) torsion (see Table S2 in the Supporting Information). The correspondence between experimental and calculated modes is supported by $H_2{}^{16}O/H_2{}^{18}O$ exchange, which does not induce any shift either in experiments (see Figure S3 in the Supporting Information) or in calculations (see Table S3 in the Supporting Information). The experimental bands at 533 (Cu^{I}) and 518 cm^{-1} (Cu^{II}) are thus assigned to contributions of the water pseudo-ligand. These results are in agreement with literature data on metal–water complexes exhibiting wagging modes of water molecules with significant intensity in the range of 650–500 cm^{-1}.[34–38]

The far-IR modes assigned to the Cu,Zn-SOD active site were used for tracking structural changes upon increasing pH value. Indeed, water IR signals are highly sensitive to hydrogen bonding interactions to neighboring groups. In Cu,Zn-SOD of bovine erythrocyte, the water molecule is included in a well-defined network of hydrogen bonds, other water molecules, and amino acid side chains.[5,6,39] This network may explain the large difference between experimental and calculated frequencies, because only the first coordination sphere of the $Cu^{II/I}$ center is taken into account in our theoretical models.

At high pH value, the Cu,Zn-SOD activity drops with a pK_a value around 10.5, but the effect of the pH value at molecular scale are still a matter of investigation. The overall shape of the far-IR difference spectrum is preserved at pH 11.6, and the structural changes mainly impact modes assigned to the water pseudo-ligand at 532 cm^{-1} (Cu^{I}) and 522 cm^{-1} (Cu^{II}), the properties of the histidine torsion modes at 652 ($Cu^{II/I}$) and 636 cm^{-1} (Cu^{I}), and a band at 277 cm^{-1} (Cu^{I}) in the absorption range of vibrations assigned to metal–histidine bonds (Figure 5). The IR band assigned to the water pseudo-ligand of Cu^{II} shifts from 518 cm^{-1} at pH 9.3 to around 522 cm^{-1} at pH 11.6, whereas the frequency of the characteristic IR modes of His side chain at 653 (Cu^{II}) and 636 cm^{-1} (Cu^{I}) is altered, reflecting an impact of the pH value on a histidine ligand both in the reduced and oxidized states.

The present FTIR data are in agreement with NMR results pointing to changes at the histidine ligands and at the water pseudo-ligand of the $Cu^{II/I}$ center. For the reduced SOD, ^{1}H NMR titration suggested that His_{61} was deproton-

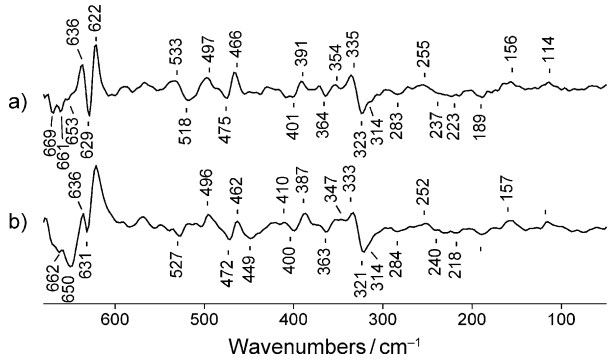

Figure 4. Low-frequency FTIR difference spectra of the reduced minus oxidized (Cu^{I}/Cu^{II}) Cu center recorded for Cu,Zn-SOD at pH 9.3 a) in H_2O and b) in D_2O.

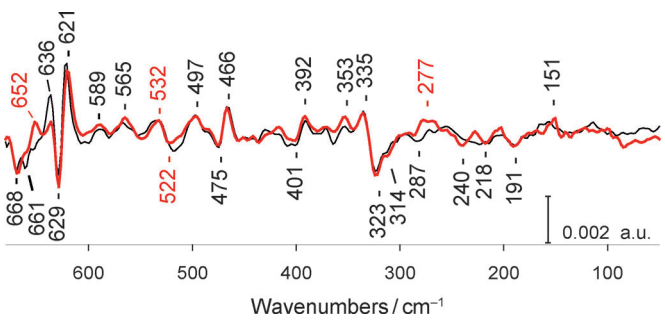

Figure 5. Comparison of the FTIR difference spectra of the reduced minus oxidized ($Cu^{I/II}$) Cu center recorded for Cu,Zn-SOD at pH 11.6 (red line) and at pH 9.3 (black line; a.u. = absorption unit).

ated at a pK_a value of 10.8[40,41], and our observation of bands increasing at 652 and 277 cm^{-1} between pH 9.3 and 11.6 is consistent with the perturbation of an histidine ligand. For the oxidized SOD, NMR investigations showed an enhancement of the ^1H and ^{17}O relaxation rates of water at alkaline pH value,[42–44] together with a weakening of the His_{46}–Cu interaction. This perturbation of His_{46} is consistent with our observation of alterations in the range of the torsion modes of histidines. These NMR results were also interpreted as signature of an hydroxide anion binding at the Cu^{II} center at alkaline pH value[11] or as an increase of the interaction between the apical water pseudo-ligand and the Cu^{II} center.[45]

Our FTIR results revisit these interpretations by questioning the deprotonation of the water pseudo-ligand. We observe that the increase in pH value results in an upshift by 4 cm^{-1} of the far-IR mode assigned to the water pseudo-ligand. We however do not observe any specific IR signature of a Cu–OH^- bond. Thus our FTIR study suggests that at pH 11.6, the water pseudo-ligand is still coordinated to the Cu^{II} center, rather than deprotonated into a hydroxide anion. The upshift of the far-IR mode indicates changes in hydrogen bonding of the coordinated water within the water network of the access channel of superoxide at high pH value. The loss in Cu,Zn-SOD activity at high pH value may result from these structural changes, together with a lower efficiency of electrostatic guidance of the $O^{2-\bullet}$ radical anion towards the Cu site.[45,46]

In conclusion, this study shows that electrochemically induced FTIR difference spectroscopy provides unique far-IR markers to track structural changes of redox-active sites for proteins in aqueous solution. This approach broadens access of far-IR spectroscopy to a large range of proteins bearing redox metal centers. This method enables thorough analysis of the properties of metal–ligand bonds, notably metal–histidine interactions often found at active sites of enzymes and absorbing below 500 cm^{-1}. For Cu,Zn-SOD, well-defined bands were detected in the far-IR region. Characteristic bands were assigned from comparison of experimental data and theoretical approach. This provides ligand side-chain and metal–ligand IR modes that characterize the metal–ligand interactions. In particular, specific signatures were identified for the Cu^{II}-His_{61}-Zn^{II} bridging motif and the water pseudo-ligand of copper. These IR modes were investigated to refine earlier mechanistic hypothesis on the conversion of the $O^{2-\bullet}$ radical anion by Cu,Zn-SOD: 1) when Cu^{II} is reduced into Cu^{I}, His_{61} decoordinates from copper and is solely bound to Zn, and 2) at alkaline pH value, the loss in catalytic activity may result from a perturbation of the network of water molecules and of the electrostatic guidance of the superoxide radical anion. This study exemplifies how this original far-IR difference technique can be used for studying the influence of various stimuli (redox potential, pH value, salinity) on metalloenzyme active sites and more generally on metal sites in solution.

Experimental Section

The complete details of the materials and methods are reported in the Supporting Information. Bovine erythrocyte Cu,Zn-SOD was used at 8 mM concentration. The electrochemical experiments were performed using a transmission electrochemical cell equipped with wedged CVD diamond windows (diameter of 10 mm and thickness of 250–350 μm).[22] The spectra were recorded at a resolution of 4 cm^{-1}, with a Bruker 66 SX spectrometer equipped with a globar as IR source, a 6 μM mylar beam splitter (Bruker) and a Si bolometer (Infrared Laboratories) provided with a 690–20 cm^{-1} filter. Single beam spectra recorded before and after a change of the applied redox potential were subtracted to calculate the difference spectra. Results obtained with 10 to 40 electrochemical cycles on the same sample were averaged to improve the signal-to-noise ratio.

Received: March 22, 2011
Published online: July 12, 2011

Keywords: density functional calculations · histidine · IR spectroscopy · proteins · terahertz

[1] I. Fridovich, *Annu. Rev. Biochem.* **1975**, *44*, 147.
[2] D. Klug-Roth, J. Rabani, I. Fridovich, *J. Am. Chem. Soc.* **1973**, *95*, 2786.
[3] G. Rotilio, R. C. Bray, E. M. Fielden, *Biochim. Biophys. Acta Enzymol.* **1972**, *268*, 605.
[4] P. J. Hart, M. M. Balbirnie, N. L. Ogihara, A. M. Nersissian, M. S. Weiss, J. S. Valentine, D. Eisenberg, *Biochemistry* **1999**, *38*, 2167.
[5] M. A. Hough, S. S. Hasnain, *Structure* **2003**, *11*, 937.
[6] D. S. Shin, M. Didonato, D. P. Barondeau, G. L. Hura, C. Hitomi, J. A. Berglund, E. D. Getzoff, S. C. Cary, J. A. Tainer, *J. Mol. Biol.* **2009**, *385*, 1534.
[7] J. A. Tainer, E. D. Getzoff, J. S. Richardson, D. C. Richardson, *Nature* **1983**, *306*, 284.
[8] V. V. Smirnov, J. P. Roth, *J. Am. Chem. Soc.* **2006**, *128*, 16424.
[9] M. Ferraroni, W. R. Rypniewski, B. Bruni, P. Orioli, S. Mangani, *J. Biol. Inorg. Chem.* **1998**, *3*, 411.
[10] J. J. P. Perry, D. S. Shin, E. D. Getzoff, J. A. Tainer, *Biochim. Biophys. Acta Proteins Proteomics* **2010**, *1804*, 245.
[11] I. Bertini, C. Luchinat, R. Monnanni, *J. Am. Chem. Soc.* **1985**, *107*, 2178.
[12] I. Bertini, C. Luchinat, M. Piccioli, M. V. Oliver, M. S. Viezzoli, *Eur. Biophys. J.* **1991**, *20*, 269.
[13] M. Paci, A. Desideri, M. Sette, M. R. Ciriolo, G. Rotilio, *FEBS Lett.* **1990**, *263*, 127.
[14] S. J. Lippard, A. R. Burger, K. Ugurbil, K. M. W. Pantoliano, J. S. Valentine, *Biochemistry* **1977**, *16*, 1136.
[15] A. E. G. Cass, H. A. O. Hill, B. E. Smith, J. V. Bannister, W. H. Bannister, *Biochemistry* **1977**, *16*, 3061.
[16] H. A. Chu, R. J. Debus, G. T. Babcock, *Biochemistry* **2001**, *40*, 2312.
[17] Y. El Khoury, A. Trivella, J. Gross, P. Hellwig, *ChemPhysChem* **2010**, *11*, 3313.
[18] Y. Kimura, A. Ishii, T. Yamanari, T.-A. Ono, *Biochemistry* **2005**, *44*, 7613.
[19] Y. Kimura, N. Mizusawa, A. Ishii, S. Nakazawa, T.-A. Ono, *J. Biol. Chem.* **2005**, *280*, 37895.
[20] Y. Kimura, N. Mizusawa, A. Ishii, T. Yamanari, T. Ono, *Biochemistry* **2003**, *42*, 13170.
[21] T. Yamanari, Y. Kimura, N. Mizusawa, A. Ishii, T.-A. Ono, *Biochemistry* **2004**, *43*, 7479.
[22] C. Berthomieu, L. Marboutin, F. Dupeyrat, P. Bouyer, *Biopolymers* **2006**, *82*, 363.
[23] L. Marboutin, A. Desbois, C. Berthomieu, *J. Phys. Chem. B* **2009**, *113*, 4492.
[24] M. A. Hough, R. W. Strange, S. S. Hasnain, *J. Mol. Biol.* **2000**, *304*, 231.

[25] J. A. Tainer, E. D. Getzoff, K. M. Beem, J. S. Richardson, D. C. Richardson, *J. Mol. Biol.* **1982**, *160*, 181.
[26] W. R. Rypniewski, S. Mangani, B. Bruni, P. L. Orioli, M. Casati, K. S. Wilson, *J. Mol. Biol.* **1995**, *251*, 282.
[27] L. Banci, I. Bertini, F. Cramaro, R. Del Conte, M. S. Viezzoli, *Eur. J. Biochemistry* **2002**, *269*, 1905.
[28] S. Hashimoto, K. Ono, H. Takeuchi, *J. Raman Spectrosc.* **1998**, *29*, 969.
[29] L. M. Murphy, R. W. Strange, S. S. Hasnain, *Structure* **1997**, *5*, 371.
[30] D. J. Wang, X. J. Zhao, M. Vargek, T. G. Spiro, *J. Am. Chem. Soc.* **2000**, *122*, 2193.
[31] K. Hasegawa, T.-A. Ono, T. Noguchi, *J. Phys. Chem. B* **2000**, *104*, 4253.
[32] K. Hasegawa, T.-A. Ono, T. Noguchi, *J. Phys. Chem. A* **2002**, *106*, 3377.
[33] N. J. Blackburn, S. S. Hasnain, N. Binsted, G. P. Diakun, C. D. Garner, P. F. Knowles, *Biochem. J.* **1984**, *219*, 985.
[34] I. Nakagawa, T. Shimanouchi, *Spectrochim Acta* **1964**, *20*, 429.
[35] K. Nakamoto, *Infrared and Raman Spectra of Inorganic and Coordination Compounds*, *Part A: Theory and Applications in Inorganic Chemistry*, 5th ed., Wiley-VCH, New York, **1997**, p. 384.
[36] V. P. Tayal, B. K. Srivastava, D. P. Khandelwal, *Appl. Spectrosc. Rev.* **1980**, *16*, 43.
[37] K. Fukushima, *Bull. Chem. Soc. Jpn.* **1970**, *43*, 1313.
[38] S. Meshitsuka, H. Takahashi, K. Higasi, *Bull. Chem. Soc. Jpn.* **1971**, *44*, 3255.
[39] M. A. Hough, S. S. Hasnain, *J. Mol. Biol.* **1999**, *287*, 579.
[40] L. Banci , I. Bertini, C. Luchinat, M. S. Viezzoli, *Inorg. Chem.* **1993**, *32*, 1403.
[41] H. A. Azab, L. Banci, M. Borsari, C. Luchinat, M. Sola, M. S. Viezzoli, *Inorg. Chem.* **1992**, *31*, 4649.
[42] I. Bertini, C. Luchinat, L. Messori, *Biochem. Biophys. Res. Commun.* **1981**, *101*, 577.
[43] N. Boden, M. C. Holmes, P. F. Knowles, *Biochem. J.* **1979**, *177*, 303.
[44] M. Terenzi, A. Rigo, C. Franconi, L. Calabrese, G. Rotilio, B. Mondovi, *Biochim. Biophys. Acta Protein Struct.* **1974**, *351*, 230.
[45] L. Banci, I. Bertini, P. Turano, *Eur. Biophys. J.* **1991**, *19*, 141.
[46] E. Argese, P. Viglino, G. Rotilio, M. Scarpa, A. Rigo, *Biochemistry* **1987**, *26*, 3224.

